C. R. Chimie 17 (2014) 681–686

Contents lists available at SciVerse ScienceDirect

Comptes Rendus Chimie

www.sciencedirect.com

Full paper/Mémoire

On the influence of the alumina precursor in Fe-K/Al_2O_3 structured catalysts for the simultaneous removal of soot and NO_x: From surface properties to reaction mechanism

Sonia Ascaso [a], María Elena Gálvez [a], Patrick Da Costa [b,*], Rafael Moliner [a], María Jesús Lázaro [a]

[a] Instituto de Carboquímica, CSIC, Miguel Luesma Castán 4, 50018 Zaragoza, Spain
[b] Institut Jean-Le-Rond-d'Alembert, UPMC Paris-6, UPMC Sorbonne Universités, CNRS UMR 7190, 2, place de la Gare-de-Ceinture, 78210 Saint-Cyr-l'École, France

ARTICLE INFO

Article history:
Received 15 May 2013
Accepted after revision 6 August 2013
Available online 17 September 2013

Special issue dedicated to François G. Garin.

Keywords:
Alumina precursor
$DeNO_x$
Soot combustion
Exhaust gas
Catalyst preparation

ABSTRACT

Cordierite-monolith supported Fe-K/Al_2O_3 catalysts were prepared using different alumina precursors. The catalysts were physico-chemically characterized, and their activity in the simultaneous removal of soot (carbon black) and NO_x was assayed with the aim of studying the influence of the particular features of each alumina precursor on the final properties of the different prepared catalyst. Structural and textural characteristics of the catalytic layer were found to be strongly dependent on the type of alumina used, which, in turn, determined the mobility of the alkali compound. This fact together with the weaker interaction of the catalytic phase with the alumina resulted in easier K diffusion and loss in some cases, whereas, on the other hand, a stronger interaction and favorable textural features of the layer resulted in notably enhanced catalytic activity.

1. Introduction

Diesel engines represent an important fragment of the light-duty vehicle market in Europe due to their excellent durability and low fuel consumption. Their main drawback is that the particular features of fuel combustion under lean conditions result in significant emissions of soot and nitrogen oxides (NO_x), which seriously hazard human health and the environment. The concern on this pollution problem has resulted in the introduction of each time more stringent legislation, limiting the emission of such contaminants [1].

Engine modifications have been introduced in the last decades in order to meet the previously existing legislative demand. However, the use of after-treatment technologies has become nowadays mandatory in order to meet the upcoming emission standards. Three ways catalysts, widely used in spark-ignition gasoline engines, are not efficient under the excess of oxygen typical of diesel engine combustion [2]. With the aim of mitigating the emission of NO_x under such oxidative conditions, two main technologies have been considered in the last years, namely Selective Catalytic Reduction (SCR) [3] and NO_x Storage Reduction (NSR). However, both alternatives still suffer from serious drawbacks in view of their effective implantation.

On the other hand, a well-established technology to eliminate soot from the exhaust is the particulate trap. This system requires the continuous oxidation of the deposited material in order to maintain an adequate engine operation [4]. Oxidation can be accomplished either by heating up the trap to an adequate temperature for soot

* Corresponding author.
E-mail address: patrick.da_costa@upmc.fr (P. Da Costa).

1631-0748/$ – see front matter
http://dx.doi.org/10.1016/j.crci.2013.08.001

oxidation over 1000 °C, or in the presence of a catalyst, which brings down the oxidation temperature to a range as close as possible to the exhaust gas exiting temperatures [5,6]. The "continuously regenerating-trap" (CRT) technology makes use of a Pt-supported catalysts upstream the particulate filter, allowing partial conversion of NO to NO_2, which is highly reactive with the soot retained in the filter [7], therefore, enhancing its oxidation.

Simultaneous removal of soot and NO_x using a single device has been previously considered. When using noble metal-based catalytic systems, like in CRT technology, only partial reduction of NO_2 to NO can be achieved, with only small amounts of NO_x converted to N_2. On the other hand, some other studies report successful NO_x conversion to N_2 [8–13] in the presence of non-noble metal compounds, i.e. such as Cu, Co and V oxides together with K-species as the alkali promoter [14]. Cobalt oxides appeared to be the most active among this series, however, its utilization in mobile applications is strongly discouraged due to its intrinsic toxicity. Iron has been successfully used as an active phase in several similar reduction–oxidation catalysts [15–17]. Its low price and innocuous chemical properties make of it an interesting option for the preparation of such catalytic systems.

The aim of the present work is to characterize the physico-chemical features and evaluate the activity of cordierite-monolith supported Fe:K/Al_2O_3 catalysts, studying the influence of the type and features of different alumina precursors on their efficiency in the simultaneous soot and NO_x removal under oxidation conditions, considering as well as the implications on the reaction mechanism.

2. Experimental

2.1. Catalysts preparation and characterization

Cylindrical shaped cordierite-monoliths ($2MgO{\cdot}2Al_2O_3{\cdot}5SiO_2$, Corning, 400 psi, 1×2.5 cm), were coated using different suspensions prepared by sol-gel synthesis. Alumina suspensions were prepared by sol-gel synthesis, using three types of highly dispersible boehmites as precursors: Disperal, Dispal 23N4-80 and Disperal P2, all of them were supplied by Sasol. Table 1 shows the more remarkable features of these alumina precursors (as provided by Sasol GmbH).

Fe ($Fe(NO_3)_3{\cdot}9H_2O$) was added to the alumina suspensions together with potassium (KNO_3) as the alkali promoter. Metal to promoter mass ratio was fixed in 5:10, for an alumina load of 5% wt., and HNO_3/Al_2O_3 ratio of 0.1. The mixtures were stirred for 24 h; measuring afterwards viscosity and pH. pH measurement was repeated after 4 days ageing time, once the suspension was stabilized. Coating was performed by forced circulation of the suspensions through the channels of the monoliths with the help of a peristaltic pump. After 30 min of circulation time, monoliths were dried in a rotating oven at 60 °C during 24 h, and subsequently calcined at 450 °C for 4 h.

Physico-chemical characterization of the prepared catalysts was performed by means of scanning electron microscopy (SEM, Hitachi S-3400 N), and N_2 adsorption at −196 °C (Micromeritics ASAP 2020), applying BET method for the determination of surface area, BJH and *t*-plot methods for the calculation of meso- and micropore volume. The adhesion of the washcoat to the cordierite-monolith was evaluated by immersing the catalytic filters in a glass vessel containing *n*-heptane and submitting them to ultrasonic agitation in an ultrasonic bath (Medi II Pselecta), during three consecutive periods of 30 min. Weight loss after each agitation period was calculated and registered.

2.2. Activity tests

Prior to the determination of the activity of the prepared catalysts, soot filtration was simulated by means of incorporating a model carbon compound (Elftex 430, Cabot). Each coated monolith was introduced for 1 min into a continuously stirred dispersion of 0.2 g of carbon black in 100 mL of *n*-pentane, removed and dried at 65 °C during 1 h. The amount of carbon black loaded corresponded approximately to 20% wt load, with respect to the mass of the catalytic material deposited on the surface of the monolith. As a result of this procedure, loose contact between soot and catalyst is obtained, which is more representative of the real contact between the soot and the catalyst at the exit exhaust of an engine [18–20].

The catalytic activity of the filters in the simultaneous removal of soot and nitrogen oxides was assayed by means of dynamic experiments, in a fixed-bed lab-scale set-up. A reactant gas containing 500 ppmv NO and 5% O_2 in Ar was flowed at 50 mL/min through a catalytic filter of 1 cm of diameter and 3 cm of length. Temperature was increased from 250 to 650 °C, at a heating rate of 5 °C/min. The concentrations of the different compounds in the exiting gas were analyzed in a mass spectrometer (Balzers 422), CO and CO_2 additionally by gas chromatography (Varian Micro GC CP 4900).

The reaction extent for NO reduction, X_{NO}, was calculated as follows, using the molar concentrations of NO in the reactant gas and in the gas exiting the catalytic reactor:

$$X_{NO} = m_{NO}/m^{i}_{NO} \quad (1)$$

Table 1
Textural and structural properties of the different alumina precursors used.

	Particle size (d50) (μm)	Surface area (S_{BET}) (m^2/g)	Pore volume (mL/g)	Crystallite size [120] (nm)	Dispersed particle size (nm)
Disperal	25	180	0.5	10	80
Dispal 23N4-80	50	200	0.4	9	90
Disperal P2	45	260	0.5	4.5	25

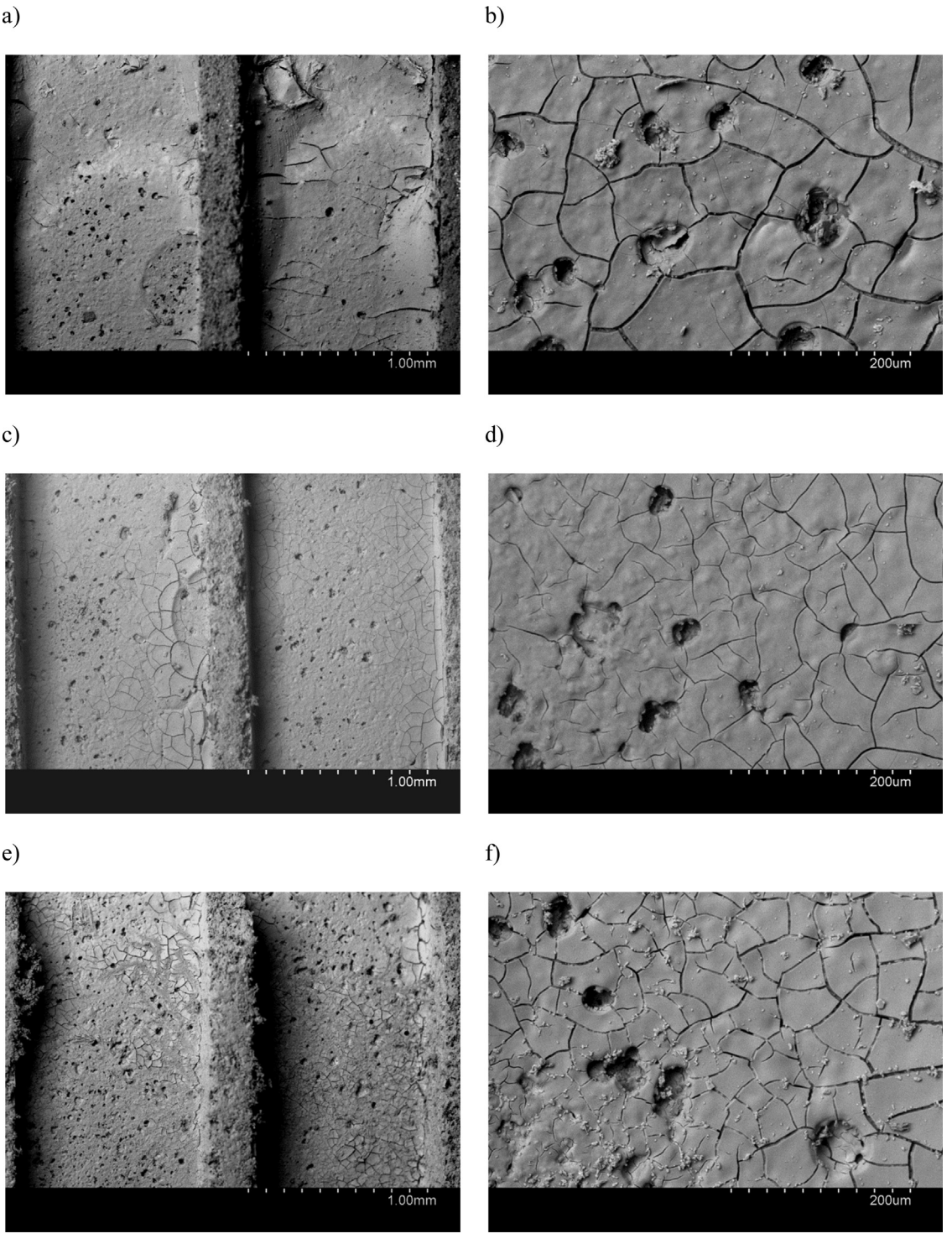

Fig. 1. SEM images for (a) and (b) FeK/P2; (c) and (d) FeK/DL; and (e) and (f) FeK/D.

Table 2
Catalyst labeling, suspension viscosity (at shear rate 1 s^{-1}) and pH after 10 days ageing time, as well as weight increase upon monolith coating.

Catalyst	Alumina precursor	Viscosity (mPa·s)	$pH_{24\ h}$	$pH_{10\ days}$	% Weight increase after coating
FeK/P2	Disperal P2 (P2)	21 618	1.67	2.8	8.3
FeK/DL	Dispal 23N4-80 (DL)	2983	1.21	1.5	9.4
FeK/D	Disperal(D)	3704	1.37	1.6	9.4

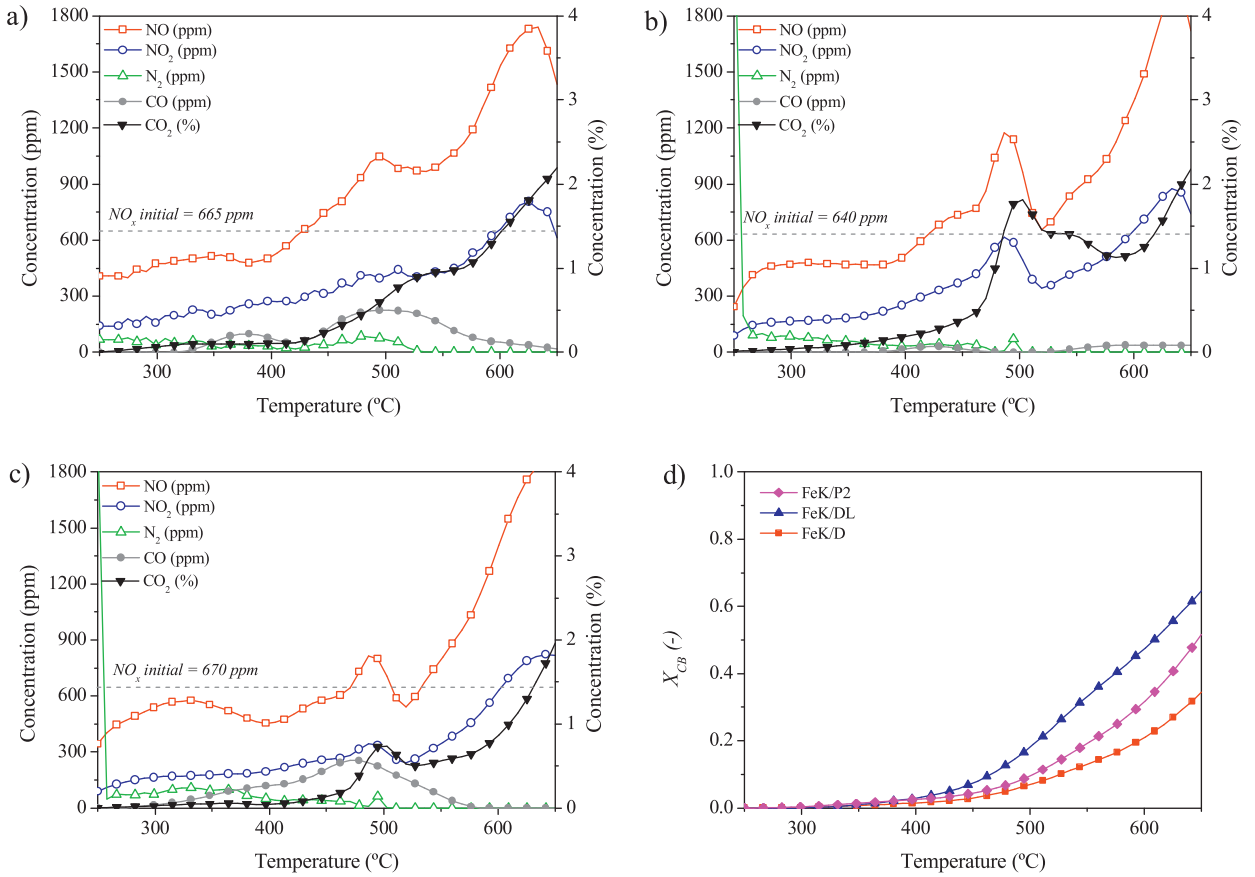

Fig. 2. Activity tests results. Concentration profiles as a function of temperature during the simultaneous removal experiments in the presence of the (a) FeK/P2, (b) FeK/DL and (c) FeK/D catalysts; and (d) carbon black conversion as a function of temperature measured during these series of experiments.

where m^i_{NO} and m_{NO} represent the initial and time t concentrations of NO, respectively. Soot conversion was calculated using the initial amount of carbon black deposited on the catalytic filter and the molar concentrations of CO and CO_2 measured in the outlet stream:

$$X_{soot} + (m_{CO_2} + m_{CO})/m^i_{soot} \quad (2)$$

where m^i_{soot} stands for the initial amount of carbon black loaded onto the catalyst.

The concentrations of CO and CO_2, m_{CO} and m_{CO_2}, were determined with the aid of the gas chromatograph, the concentrations of NO, NO_2 and N_2 were calculated from the data registered by the mass spectrometer, taking into account all the possible contributions an interactions of the rest of the components in the gas mixtures to their corresponding m/z values of 30, 46 and 28. N_2O formation was assessed by means of comparing the concentration of CO_2 measured by gas chromatography and the concentration obtained from the m/z 44 intensity measured by mass spectrometry.

3. Results and discussion

Table 2 lists the different catalysts prepared, their labelling, as well as the corresponding coating suspension, their viscosity and pH. Weight increase upon the incorporation of the catalytic layer is also presented in Table 2. As previously reported [14], the use of the different alumina precursors notably influences the suspension stabilization pH and viscosity, pointing to differences in the gelation process. This is mostly a consequence of the different precursor's particle size and surface area. In this sense, the dispersion prepared using Disperal P2 yields higher viscosity values in comparison with the dispersions prepared using Dispal and Disperal, due to the lower dispersed particle size of Disperal P2, resulting in a fast gelation process.

Moreover, the viscosity of the dispersion strongly influences the final coating of the monolith surface, as well as the thickness of the deposited layer. Fig. 1 shows the SEM images acquired for the three catalysts prepared using the different alumina precursors. SEM analysis confirmed an adequate and quite homogeneous coating of the cordierite surface. However, some differences in the morphology of the catalytic layer can be observed.

Cracks are formed normally as a consequence of catalyst drying and calcination [3,21]. Bigger particle size will result in less mechanical strain within the packed alumina particles constituting the layer, particularly upon such thermal treatments. Crack formation is thus expected to depend on the degree of particle packing in the catalytic layer, which will mostly be determined by the alumina

Table 3
Weight loss (%) measured after adherence test for the different catalysts prepared.

	% Weight loss after 30 min	% Weight loss after 60 min	% Weight loss after 90 min
FeK/P2	15.3	19.5	20.2
FeK/DL	5.1	6.4	6.4
FeK/D	3.5	4.7	4.8

Table 4
K and Fe analysis by means of SEM–EDX, in the different catalysts prepared.

Catalyst	Spot	1	2	3	4	Average
FeK/P2	% Wt K	7.01	7.65	6.85	6.24	6.93
	% Wt Fe	4.41	4.30	3.79	4.02	4.13
FeK/DL	% Wt K	6.84	6.20	5.35	4.89	5.82
	% Wt Fe	1.72	1.85	1.57	2.30	1.86
FeK/D	% Wt K	26.47	26.02	24.66	28.39	26.38
	% Wt Fe	7.27	6.72	7.55	5.24	6.69

precursor particle and/or dispersed size, as well as on the suspension properties, which will yield different layer thicknesses. SEM shows lower tendency towards the formation of cracks in the FeK/DL catalyst prepared using Dispal 23N4-80 as the precursor. This is in agreement with its higher particle (50 μm) and dispersed size (90 nm) in this series of materials. However, layer thickness also plays a role. SEM observation allowed the measurement of average layer thicknesses, between 10 and 25 μm. Thicknesses were all the time lower in the case of the FeK/DL and FeK/D catalysts, in comparison to the FeK/P2 one. This is due to the lower viscosity of the suspensions prepared using Dispal 23N4-80 and Disperal as the precursors, whereas for Disperal P2 much higher viscosity led to a less uniform coating, resulting in excessive accumulation of catalytic layer in some areas, as can be appreciated in Fig. 1 a.

Weight loss measured after the adherence tests confirm SEM observations. In fact, the catalyst prepared using the P2 precursor shows less stable coating with the highest tendency to detach from the cordierite walls (Table 3).

EDX analysis was performed on selected spots on SEM images. The results of such analyses are shown in Table 4. Note that Fe and K contents may vary within the same catalyst also as a consequence of its relative heterogeneity and due to the intrinsic confined nature of EDX analysis, which always refers to a very small portion of sample area. It is clear, however, that the surface of the FeK/D catalysts is particularly enriched in K, with contents over 25% wt. This is not observed for FeK/P2 and FeK/DL. Coming back to SEM images, Fig. 1f evidences the presence of K exiting through the cracks on the layer structure, see the small lighter contrast deposits having different morphology of that of the alumna layer, in agreement with the increased presence of the alkali compound on the surface of this FeK/D catalyst. Potassium reaches the surface and diffuses through the cracks and pores due to the formation of a K_2O metastable liquid-solid phase upon heating, i.e. during catalyst calcination [11,22]. The textural and structural properties of the catalytic layer determine the extent to which the alkali reaches its surface.

Table 5 presents the results of the textural characterization of the catalysts by means of N_2 adsorption, either on their powder formed or once supported on the cordierite-monolith. All the materials can be considered as mostly mesoporous, with almost no presence of micropores. Pore and mesopore volume are lower in the P2-based catalysts than in the rest of the series. Moreover, the average pore size in these materials is 3.2–3.7 nm, which is much lower than in the D or DL-based catalysts. These particular textural features in the case of FeK/P2 will explain the lower ability of the K compound to diffuse to the upper part of the catalytic layer, observed by means of SEM–EDX analysis. However, the very similar textural features of the catalytic layer in FeK/DL and FeK/D do not provide any explanation for the easier diffusion of K in the case of the latter. Given that the structural characteristics of the catalytic layer do not differ too much as well among these catalysts, this fact points thus to a stronger chemical interaction of the alkali compound with the alumina support in the case of FeK/DL which does not occur for FeK/D.

Table 5
Surface area (S_{BET}), pore volume (V_{pore}) and mesopore (V_{BJH}) volume, as well as average pore size derived from N_2 adsorption isotherms for the different catalysts.

	S_{BET} (m^2/g)	V_{pore} (cm^3/g)	V_{BJH} (cm^3/g)	Average pore size (nm)
FeK/P2 (powder)	78.0	0.071	0.066	3.2
FeK/P2 (monolith)	9.8	0.011	0.011	3.7
FeK/DL (powder)	82.9	0.170	0.180	5.9
FeK/DL (monolith)	9.2	0.019	0.020	6.7
FeK/D (powder)	89.4	0.161	0.182	5.3
FeK/D (monolith)	8.3	0.015	0.016	6.1

Fig. 2 shows the results obtained in the simultaneous removal activity tests performed in the presence of FeK/P2, FeK/DL and FeK/D catalysts. In Fig. 2a, b and c, the concentrations of NO_x, N_2, CO and CO_2 are plotted as a function of temperature. In all cases, NO_x concentration decreases first at temperatures from 250 to 425 °C due to the adsorption of these nitrogen species on the catalyst surface. NO_2 concentration measured within this interval, not plotted in Fig. 2 for the sake of clarity, decreases in parallel to that of NO. Adsorption is further confirmed by closing the N-balance, taking into account that no N_2 corresponding to the reduction of NO_x species was measured within this temperature window. At temperatures higher than 425 °C, nitrogen species start desorbing from the surface of the catalyst. Consequently, evolution of NO and NO_2 is observed in each plot. Note that part of this NO_x evolution (up to 5%, as evidenced in TPD experiments) may correspond to the thermal decomposition of nitrate species remaining from catalyst preparation due to their incomplete calcination. The evolution of NO_x corresponds to an increase in CO_2 concentration, pointing to the real set-off for carbon black oxidation, enhanced by the presence of NO_2 in the gas. At the same time, NO and NO_2 concentration decrease within the temperature range 500–550 °C, to finally increase again until the end of the experiment at 650 °C. Enhanced soot oxidation in the presence of NO_2 was previously reported in [14]. In the absence of NO in the reactant gas, the set-off for soot oxidation was delayed by 50 °C with respect to the experiment performed in the presence of 500 ppmv of NO.

Differences in the concentration profiles registered here are due to different activities of the three prepared catalysts. As it can be observed in Fig. 2d, the highest oxidation rate, as well as the highest final carbon black conversion, is obtained in the presence of FeK/DL. This corresponds well with the more marked evolution of CO_2 shown in Fig. 2b and can be also related to the highest extent of NO formation and desorption registered in the presence of this catalyst. Moreover, oxidation is more selective towards CO_2 formation than for the rest of the catalysts in this series, with almost negligible amounts of CO formed during the reaction. Furthermore, from 500 to 550 °C, the NO_x consumption occurs to a greatest extent as well in the presence of FeK/DL, pointing to this catalyst as the most effective in the simultaneous removal process.

The mobility of the alkali promoter plays for sure an important role in the catalytic activity. Therefore, the lower activity of the catalyst prepared using the P2 alumina might be ascribed to the lower presence of the K compounds on the surface of the catalyst, related to the particular textural properties of the catalytic layer, i.e. lowest average pore size and pore volume. In the opposite case, the lowest activity, particularly towards carbon black oxidation, determined for FeK/D may be ascribed to a certain and non-negligible loss of potassium during both catalyst preparation and reaction, which is favored by the bigger pore size and higher pore volume in comparison to the P2-based catalyst (Tables 4 and 5). Moreover, the weaker interaction of K with the alumina in the case of this D-based catalyst additionally facilitates the diffusion and loss of alkali promoter in this case.

4. Conclusions

Cordierite-monolith supported Fe-K/Al_2O_3 catalysts were prepared using three different alumina precursors. Their activity was assayed in the simultaneous removal of soot (carbon black) and NO_x. The use of different alumina precursors results in different coating morphologies and catalytic layers, possessing different textural properties.

Both Disperal (D) and Dispal (DL) alumina precursors result in good layer adherence and, particularly, Dispal (DL), in lower tendency towards the formation of cracks. On the other hand, Disperal P2 (P2) alumina catalyst presented a less uniform and less stable coating of the cordierite surface.

Both structural and textural properties determine the mobility of K and its diffusion towards the surface of the deposited catalytic layer. Higher number of cracks as well as higher pore volume and average diameter resulted in a considerable easier diffusion of the alkali out of the layer. Stronger interaction of the alkali with the alumina in the case of the Dispal (DL)-based catalyst prevented the loss of alkali, yet, permitting its mobility, resulting in the highest catalytic activity in the simultaneous removal reaction.

Acknowledgements

S. Ascaso thanks CSIC for her JAE doctoral grant. M.E. Gálvez is indebted to the Spanish Ministry of Economy and Competitiveness (Secretaría de Estado de I+D+I, previously MICINN) for her Ramón y Cajal contract.

References

[1] Regulation EC N. 715/2007.
[2] D. Fino, N. Russo, C. Baldini, G. Saracco, V. Specchia, AIChE J. 8 (2003) 2173.
[3] A. Boyano, M.J. Lázaro, C. Cristiani, F.J. Maldonado-Hodar, P. Forzatti, R. Moliner, Chem. Eng. J. 149 (2009) 173.
[4] P. Zelenka, W. Cartellieri, P. Herzog, Appl. Catal. B: Environ. 10 (1996) 3.
[5] P. Ciambelli, V. Palma, P. Russo, S. Vaccaro, Catal. Today 73 (2002) 363.
[6] B.R. Stanmore, J.F. Brilhac, P. Gilot, Carbon 39 (2001) 2247.
[7] B.J. Cooper, J.E. Thoss, SAE Paper 890404, 1989.
[8] K. Hizbul, S. Kureti, W. Weisweiler, Catal. Today 93 (2004) 839.
[9] N. Nejar, M.J. Illán-Gómez, Appl. Catal. B: Environ. 70 (2007) 261.
[10] D. Fino, P. Fino, G. Saracco, V. Specchia, Appl. Catal. B: Environ. 43 (2003) 243.
[11] V.G. Milt, E.D. Banús, M.A. Ulla, E.E. Miró, Catal. Today 133 (2008) 435.
[12] H. Lin, Y. Li, W. Shangguan, Z. Huang, Comb. Flame 156 (2009) 2063.
[13] W.F. Shangguan, Y. Teraoka, S. Kagawa, Appl. Catal. B: Environ. 16 (1998) 149.
[14] M.E. Gálvez, S. Ascaso, I. Tobías, R. Moliner, M.J. Lázaro, Catal. Today 191 (2012) 96.
[15] M.L. Cubeiro, H. Morales, M.R. Goldwasser, M.J. Pérez-Zurita, F. González-Jiménez, C.N. Urbina de, Appl. Catal. A: Gen. 189 (1999) 87.
[16] B.C. Enger, R. Lodeng, A. Holmen, Appl. Catal. A: Gen. 346 (2008) 1.
[17] C.W.B. Bezerra, L. Zhan, K. Lee, H. Liu, A.L.B. Marques, E.P. Marques, H. Wang, J. Zhang, Electrochim. Acta 53 (2008) 4937.
[18] J.P.A. Neeft, M. Makkee, J.A. Moulijn, Appl. Catal. B: Environ. 8 (1996) 57.
[19] J.P.A. Neeft, M. Makkee, J.A. Moulijn, Appl. Catal. B: Environ. 12 (1997) 21.
[20] E.D. Banús, V.G. Milt, E.E. Miró, M.A. Ulla, Appl. Catal A: Gen. 379 (2010) 95.
[21] M. Valentini, G. Groppi, C. Cristiani, M. Levi, E. Tronconi, P. Forzatti, Catal. Today 69 (2001) 307.
[22] R. Matarrese, L. Castoldi, L. Lietti, P. Forzatti, Catal. Today 136 (2008) 11.